

# The Physico-Chemistry of Adhesions of Protein Resistant and Weak Polyelectrolyte Brushes to Cells and Tissues

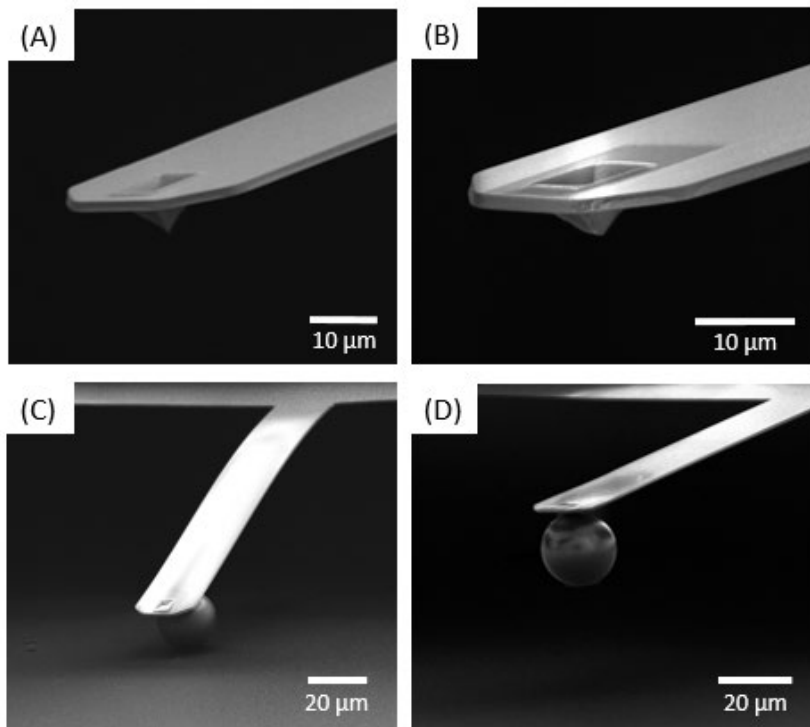
## Supplementary Information

*Edward J. Cozens,<sup>1,2</sup> Dexu Kong,<sup>1,2</sup> Nima Roohpour<sup>3</sup> and Julien E. Gautrot<sup>1,2\*</sup>*

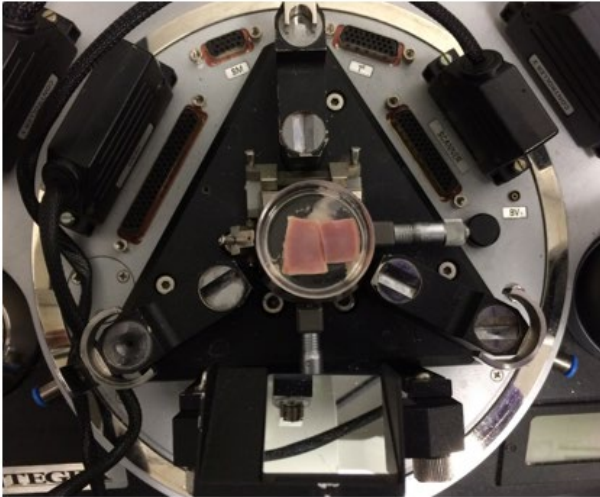
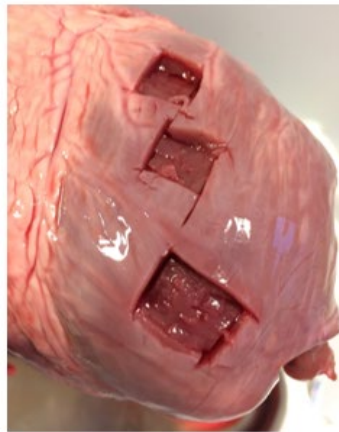
*<sup>1</sup>Institute of Bioengineering and <sup>2</sup>School of Engineering and Materials Science, Queen Mary, University of London, Mile End Road, London, E1 4NS, UK.*

*<sup>3</sup>Consumer Healthcare R&D, GlaxoSmithKline, St George's Avenue, Weybridge, Surrey, KT13 ODE, UK.*

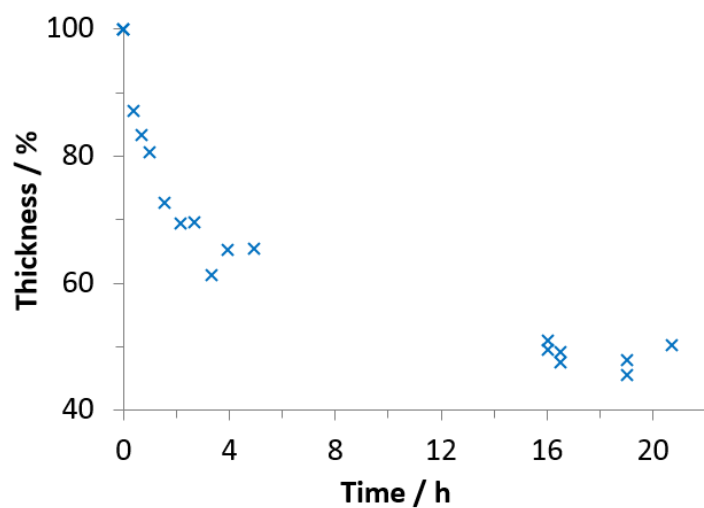
*\*Corresponding author. [j.gautrot@qmul.ac.uk](mailto:j.gautrot@qmul.ac.uk)*



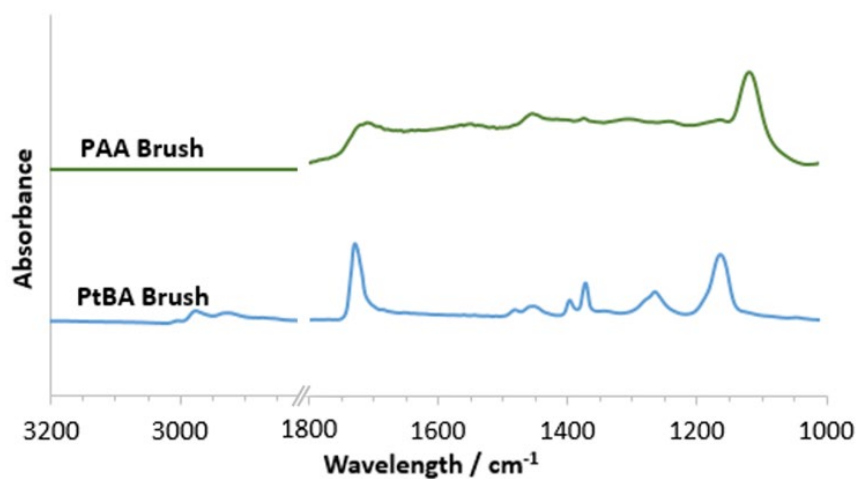
**Supplementary Figure S1.** Sequence of steps used for the fabrication of colloidal probe cantilevers. (A) Rectangular cantilever with sharpened tip, as purchased from the manufacturer. (B) An integrated FIB was used to remove a portion from the end of the tip, providing a more effective surface for the placement of the bead. (C) The end of the tip was dipped into glue and then brought into contact with the surface of a bead that had been deposited on a silicon wafer. A high current (1-3 nA) was focussed at the glue for several minutes, resulting in curing of the glue and creation of a strong bond between the tip and bead. (D) The resulting colloidal AFM probe was then removed from the surface, ready for AFM measurements. All images were acquired using a Scanning Electron Microscope (Quanta 3D FEG, FEI, EU/USA).

**A****B****C**

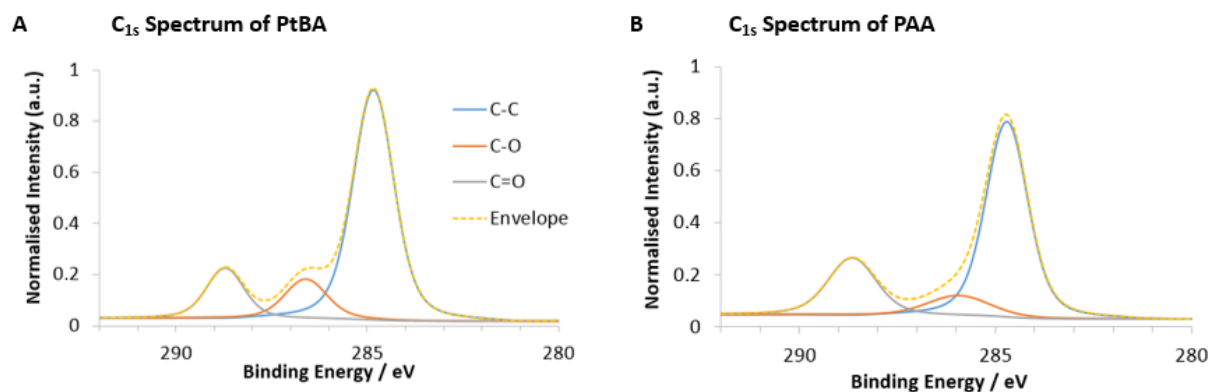
**Supplementary Figure S2.** Dissection and preparation of porcine tissues for AFM. (A) Loading of epicardial samples in the AFM. Following dissection samples were glued in place within petri dishes and submerged in PBS. (B) Example of dissection location for keratinized gingiva samples. (C) Example of dissection locations for epicardial samples.



**Supplementary Figure S3.** Reduction in dry ellipsometric thickness of PtBA brushes during the deprotection of t-butyl esters. PtBA brushes were immersed in a solution of dichloromethane/trifluoroacetic acid solution (10:1 v/v) at room temperature overnight. Thickness values are given as a percent of the original thickness.



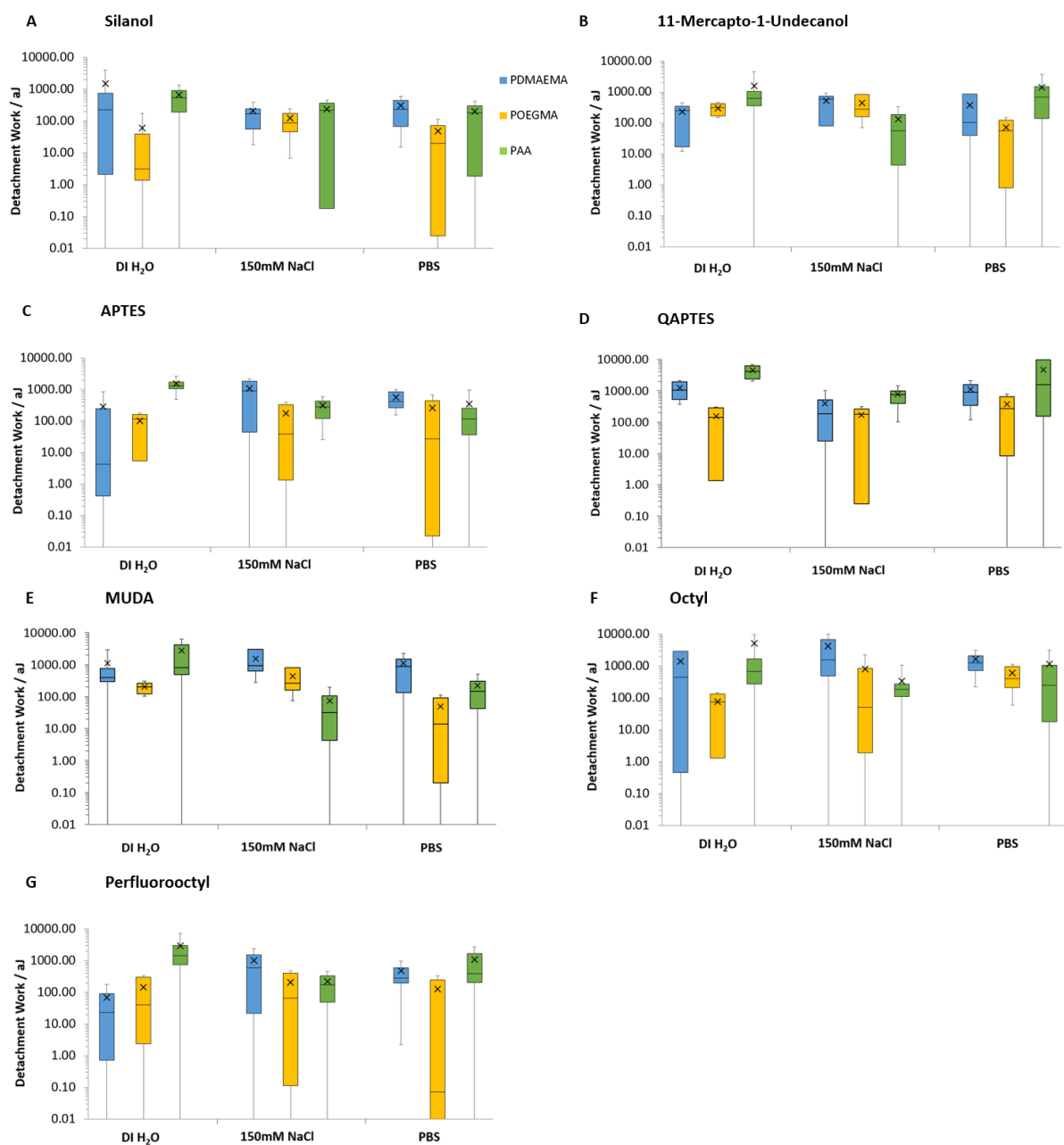
**Supplementary Figure S4.** FTIR characterisation of PtBA brushes before and after deprotection. The full conversion of the brushes to PAA is represented by the clear disappearance of the tert-butyl bending bands at 2976, 1392 and 1367  $\text{cm}^{-1}$ , and the shift (and broadening) of the carbonyl band from 1730 to 1712  $\text{cm}^{-1}$ .



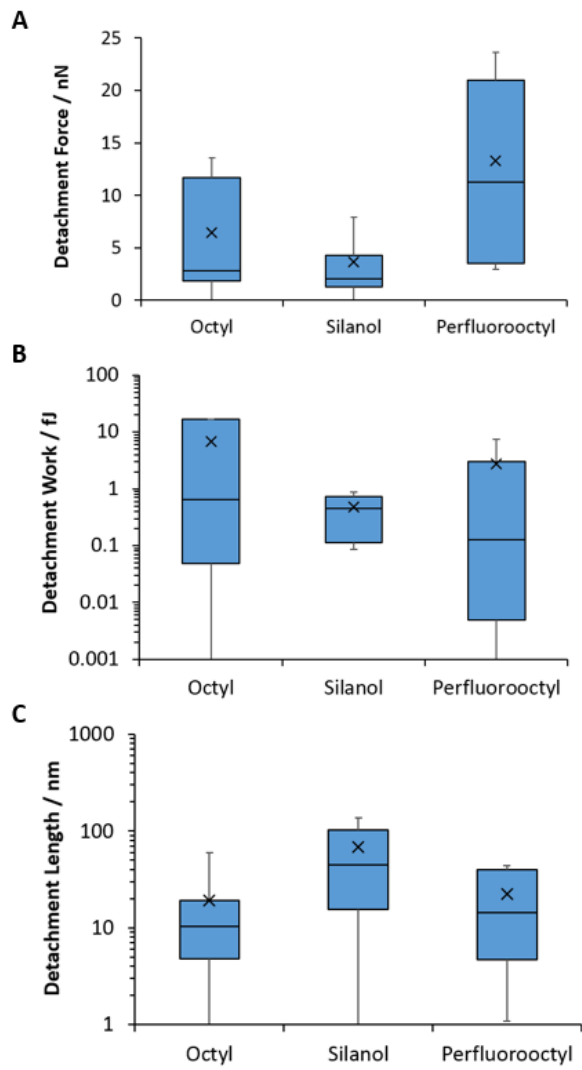
**C Survey Scan Peaks**

Element and its orbital	Atomic %		Binding Energy / eV	
	PtBA	PAA	PtBA	PAA
C <sub>1s</sub>	79.56	68.37	285.51	285.48
O <sub>1s</sub>	20.44	31.63	533.02	532.96

**Supplementary Figure S5.** XPS spectra for the characterisation of PtBA and PAA planar polymer brush surfaces. (A) High-resolution deconvoluted spectra for PtBA C<sub>1s</sub> signals. (B) High-resolution deconvoluted spectra for PAA C<sub>1s</sub> signals. (C) Atom composition (C<sub>1s</sub> and O<sub>1s</sub>) and corresponding binding energies of the main peaks measured for PtBA and PAA brushes.

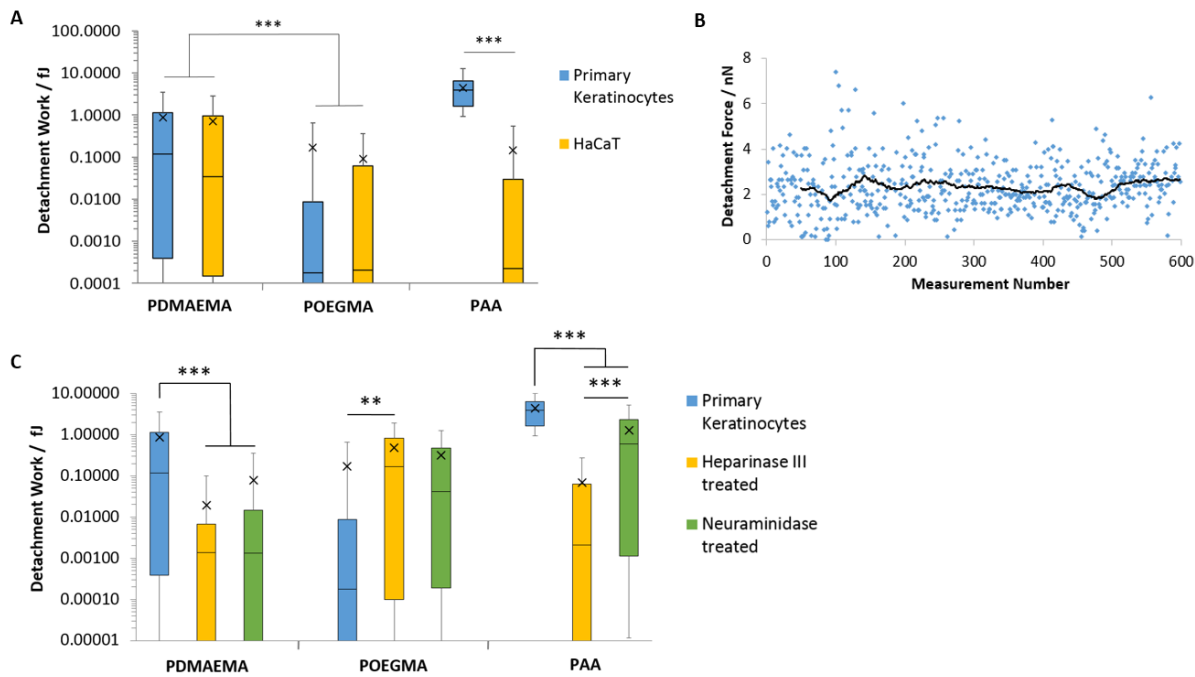


**Supplementary Figure S6.** Detachment work measured for the adhesion of PAA, PDMAEMA and POEGMA brushes to hydroxyl-terminated, charged and hydrophobic monolayers. (A) Silanol monolayers. (B) 11-Mercapto-1-undecanol monolayers assembled on gold. (C) Ammonium (APTES) monolayers. (D) Quaternary ammonium (QAPTES) monolayers. (E) Undecanoic acid (MUDA) monolayers assembled on gold. (F) Octyl monolayers. (G) Perfluorooctyl monolayers.



**Supplementary Figure S7.** Detachment force (A), work (B) and length (C) measured for the adhesion of PAA brushes to hydrophobic (octyl and perfluorooctyl) and hydrophilic (silanol) monolayers submerged in deionised water.





**Supplementary Figure S8.** Characterisation of adhesive interactions between polymer brushes and cell monolayers. Testing was carried out on samples submerged in PBS. (A) Detachment work for primary keratinocyte (PK) and HaCaT cell monolayer adhesion. (B) Variation of PAA detachment force during repeated measurements on a primary keratinocyte cell sheet as a function of time. The black line illustrates a 50 point moving average of the data. (C) Detachment work between polymers and primary keratinocyte monolayers with and without enzymatic treatment. Data is plotted as means, with box plots. \*\*,  $p \leq 0.01$ . \*\*\*,  $p \leq 0.001$ .

**Supplementary Table S1.** Contact angle measurements of deionised water droplets (3  $\mu$ L) deposited at the surface of SAMs and polymer brushes, assembled on either gold or silicon substrates. Ellipsometric thicknesses of corresponding surfaces are also given. PAA brushes correspond to a polymerization time of 6 h.

Surface Functionalisation	Substrate Material	Contact Angle	Thickness / nm
Silanol	Silicon	$14.2 \pm 3.1^\circ$	$1.1 \pm 0.1$
APTES	Silicon	$37.7 \pm 3.0^\circ$	$1.8 \pm 0.1$
QAPTES	Silicon	$21.5 \pm 1.2^\circ$	$1.8 \pm 0.1$
Octyl	Silicon	$96.3 \pm 1.3^\circ$	$2.3 \pm 0.2$
Perfluorooctyl	Silicon	$103.7 \pm 1.4^\circ$	$1.5 \pm 0.1$
PtBA Brush	Silicon	$87.0 \pm 0.6^\circ$	$69.7 \pm 3.8$
PAA Brush	Silicon	$37.4 \pm 0.7^\circ$	$34.3 \pm 2.7$
11-Mercapto-1-undecanol	Gold	$32.5 \pm 2.8^\circ$	$1.6 \pm 0.1$
MUDA	Gold	$50.3 \pm 0.9^\circ$	$1.7 \pm 0.1$